

Palladium(II) and Platinum(II) Mononuclear Complexes and Tendency to Undergo Dehydrogenation of the Multiple N-Donor Ligand Di-(2-pyridyl)dihydropyrazine

Edoardo Raciti, Maria Pia Donzello,* Elisa Viola, Mauro Bassetti,* Ida Pettiti, Noemi Bellucci, Corrado Rizzoli,* and Claudio Ercolani*



Cite This: <https://dx.doi.org/10.1021/acs.inorgchem.0c00699>



Read Online

ACCESS |



Metrics & More

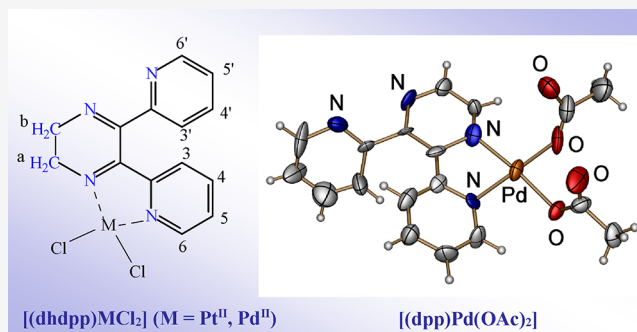


Article Recommendations



Supporting Information

ABSTRACT: The already known di(2-pyridyl)dihydropyrazine (dhdpp) was prepared and isolated also in the form of a bis-hydrated species, i.e., dhdpp·2H₂O. As established by X-ray work, a small amount of single crystals of di(2-pyridyl)-pyrazine (dpp) was also obtained from the mother liquors, this testifying the possibility of a dehydrogenation process dhdpp → dpp in the absence of a catalyst. Using dhdpp as a ligand, mononuclear metal derivatives of formula [(dhdpp)MCl₂]*x*H₂O (M = Pd^{II}, Pt^{II}) were obtained as stable-to-air solids, studied by X-ray powder, IR, UV–visible, and ¹H NMR spectra, and proved to exhibit a N₂MCl₂ coordination site involving one pyridine and one pyrazine N atom (“py-pyz” coordination). An interesting relationship has been established in terms of the observed types of coordination with the analogs of di(2-pyridyl)-pyrazine (dpp) formulated as [(dpp)MCl₂]*x*H₂O, proved also by ¹H NMR spectra to exhibit the “py-pyz” mode of coordination. Attempts to isolate from the reaction of dhdpp with Pd(OAc)₂ the corresponding mononuclear derivatives were shown to lead, as definitely supported by ¹H NMR spectral data and crystallographic work, to the exclusive formation of the corresponding dpp complex [(dpp)Pd(OAc)₂]*x*H₂O (“py-pyz” coordination site), this proving the tendency of dhdpp to generate dpp under different reaction conditions. The promoted conversion of dhdpp into dpp in the complex was examined by sequential NMR analysis and established to be determined by Pd(OAc)₂ which plays the role of catalyst. The new salt-like species [(CH₃)(dhdpp)PdI₂](I)·7H₂O, prepared starting from [(dhdpp)PdCl₂] in its reaction with CH₃I, allowed the separation from the mother liquors of small brown crystals identified on the basis of X-ray analysis as the already known complex of formula [(dpp)PdI₂] (“py-py” coordination), this result once again outlining the tendency of dhdpp to be dehydrogenated to dpp.



INTRODUCTION

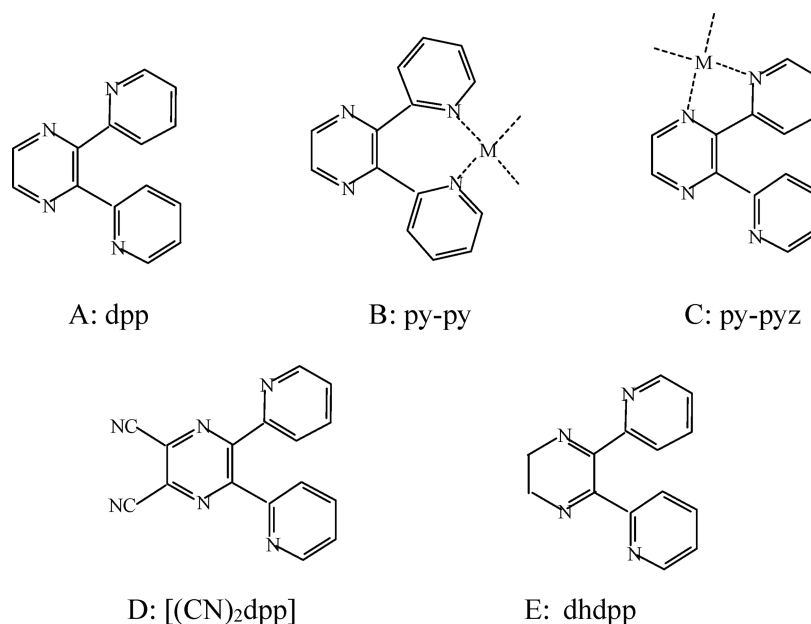
It is well known that the N donor properties of pyridine in terms of binding metal centers are stronger than those of pyrazine due to its higher basicity (pyridine, pK_a = 5.5; pyrazine, pK_a = 0.65).¹ It is of fundamental interest to investigate the coordination sites binding to a metal center in the complexes formed by multidentate N-donor ligands. The concomitant presence of two vicinal pyridine rings and one pyrazine ring in 2,3-di(2-pyridyl)-1,4-pyrazine (dpp, Chart 1A) and in related species having either open chains or annulated ring substituents in 5,6-positions has been considered as to the formation of metal derivatives during the last 60 years, and this work has been recently reviewed.² As it appears evident from the complete list of data (see Table 1 in ref 2), achieved information on mononuclear metal complexes indicates as comparable the number of complexes in which metal coordination takes place at the N atoms of the two pyridine rings (Chart 1B, “py-py” coordination) or by using one pyridine N atom and one pyrazine N atom (Chart 1C, “py-

pyz” coordination), specific coordination depending, although not exclusively, on the type and oxidation state of the metal center.

Focusing on the series of known mononuclear complexes of dpp having formula [(dpp)MX₂] with M = Pd^{II} or Pt^{II} recently reported and structurally elucidated by X-ray work (see Table 1 in ref 2), the observed types of coordination, i.e., “py-py”^{3a-f} and “py-pyz”^{3g-1} are also comparable. Our work in the area was confined to the synthesis and characterization of Pd^{II} and Pt^{II} mononuclear derivatives of a substituted dpp, i.e., 2,3-dicyano-5,6-di-(2-pyridyl)-1,4-pyrazine, [(CN)₂dpp] (Chart

Received: March 6, 2020

Chart 1. Schematic Representation of the Structure of dpp (A), [(CN)₂dpp] (D), and dhdpp (E) and of the py-py (B) and py-pyz (C) Modes of Coordination



1D). Crystallographic work on the two isostructural complexes $[\{(CN)_2dpp\}MCl_2]$ ($M = Pd^{II}, Pt^{II}$)^{4,5} (Figure 1) definitely establishes that chelation of the metal center in both species is of the type “py-py”.

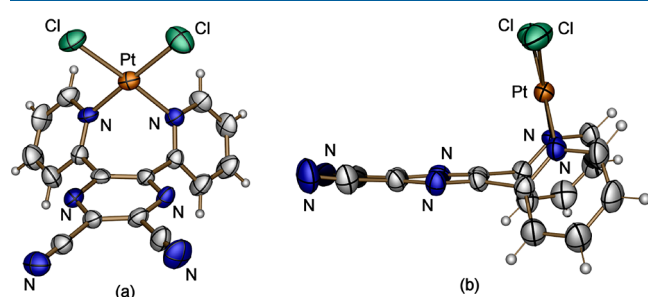


Figure 1. ORTEP front (a) and side (b) views (50% probability ellipsoids) of $[\{(CN)_2dpp\}PtCl_2]$.

In the effort to render more probable and encounter the asymmetric “py-pyz” type of chelation, attention has been focused in the present work on the formation of Pt^{II} and Pd^{II} complexes of 2,3-dihydro-5,6-di(2-pyridyl)-1,4-pyrazine (dhdpp, Chart 1E), in which the dihydropyrazine ring replaces the pyrazine ring present in dpp. Asymmetric chelation, i.e., the “py-pyz” mode of coordination, was supposedly thought to be more competitive for dhdpp by the implied enhancement of the N donor properties of the dihydropyrazine ring, and the presented results are also viewed in a comparison with those obtained in parallel species by using ligand dpp. Worth noting, the coordination properties of dhdpp are fully open to exploration, since in relation to the highly extended coordination chemistry of mono-, di-, and multinuclear dpp metal derivatives,² to our knowledge the only one so far previously reported dhdpp metal derivative is the Pt^{II} complex $[(dhdpp)PtCl_2]$,⁶ a species further explored in the present contribution.

It is of relevance to notice here that dhdpp shows a tendency, under a variety of experimental conditions, to

undergo a dehydrogenation process thus forming dpp. The driving force of this process is in relationship with the energy relaxation effect which implies for the pyrazine ring in the process $dhdpp \rightarrow dpp$ the achievement of rearomatization. The first description of this process consisting of the releasing of two hydrogen atoms taking place in hot mesitylene (1,3,5-trimethylbenzene) in the presence of a palladium/charcoal catalyst was given by the authors who first reported the synthesis of dhdpp.⁷ As it will be shown, the process $dhdpp \rightarrow dpp$ has been accurately taken into account in the present work while dealing with the synthesis of dhdpp and its related mononuclear complexes formed by its reaction with Pd^{II} and Pt^{II} reactants.

EXPERIMENTAL SECTION

Solvents and reagents were commercially obtained from Carlo Erba, Fluka, or Sigma-Aldrich and used as received unless otherwise specified. Dimethyl sulfoxide (DMSO) was freshly distilled over CaH_2 before use. 2,3-Bis(2-pyridyl)-1,4-pyrazine (dpp) and 2,2'-pyridyl were purchased from Sigma-Aldrich. $[(DMSO)_2PtCl_2]$ ⁸ and $[(C_6H_5CN)_2MCl_2]$ ($M = Pd^{II}, Pt^{II}$)⁹ were prepared as reported in the literature.

Synthetic Procedures. 2,3-Di-(2-pyridyl)-5,6-dihydropyrazine, dhdpp, and its Bis-Hydrated Derivative, $dhdpp \cdot 2H_2O$. Following the previously reported synthesis of dhdpp,⁷ a solution of ethylenediamine (1.10 mL, 9.98 mmol) in ethanol (2.40 mL) was added to a solution of 2,2'-pyridyl (2.10 g, 9.90 mmol) in the same solvent (15.0 mL). The mixture was kept to reflux in air for 1 h; during this time, the initial yellow color of the solution changed to brown red. After having been cooled to room temperature, the solution was kept in the refrigerator for 24 h, and the suspended orange crystalline material was separated by centrifugation, washed twice with ethanol, and brought to constant weight under vacuum (10^{-2} mmHg, 996.0 mg, yield 42.2%). Calcd for dhdpp, $C_{14}H_{12}N_4$: C, 71.17; H, 5.12; N, 23.71%. Found: C, 70.80; H, 5.63; N, 23.32%. IR (cm^{-1}): 3034 (w), 2982 (vw), 2941 (w), 2877 (vw), 2824 (w), 1622 (vw), 1579 (vs), 1551 (m), 1469 (m-s), 1457 (m-s), 1426 (m), 1327 (m), 1284 (w-m), 1230 (w-m), 1153 (w), 1093 (m-s), 1048 (vw), 1028 (w), 983 (vs), 891 (w), 854 (w), 814 (m), 786 (s), 753 (w), 741 (m-s), 696 (w), 623 (m), 575 (w), 559 (m-s), 498 (vw), 477 (w), 405 (m), 389 (w), 372 (w), 344 (w), 283 (s). UV-vis spectral data (λ , nm; log ϵ)

in CH₃CN: 268 (3.88), 368 (2.67); in CHCl₃: 271 (3.88), 367 (2.73). ¹H NMR (300 MHz, CDCl₃, Figure S1A): δ/ppm = 8.18 (d, J = 4.8 Hz, 2H, H₆, H_{6'}); 7.96 (d, J = 7.9 Hz, 2H, H₃, H_{3'}); 7.76 (td, J = 1.7 Hz, 7.63 Hz, 2H, H₄, H_{4'}); 7.16 (m, 2H, H₅, H_{5'}); 3.79 (s, 4H, H_a, H_b).

Crystallization of dhdpp from hot ethanol gave light orange crystals which were examined by crystallographic work. The obtained crystal data (Table S1) were found perfectly coincident with those of the structure of dhdpp recently reported.¹⁰ Further precipitate was obtained from the mother liquors kept in the refrigerator for 5–6 days. The light yellow-orange solid, separated by centrifugation, was washed with ethanol and brought to constant weight under vacuum (10⁻² mmHg, 42.6 mg); the compound was established to be the bis-hydrated dhdpp. Calcd for dhdpp·2H₂O, C₁₄H₁₆N₄O₂: C, 61.75; H, 5.92; N, 20.57%. Found: C, 62.17; H, 5.60; N, 20.29%. IR (cm⁻¹): 3312 (s), 3044 (vw), 2926 (vw), 1648 (vs), 1580 (w), 1560 (w), 1520 (vs), 1457 (m), 1427 (m), 1316 (w), 1285 (m), 1247 (m), 1219 (w), 1150 (w), 1078 (vw), 1040 (vw), 1024 (vw), 990 (m), 962 (vw), 880 (w), 815 (w), 789 (vw), 742 (m), 673 (s), 617 (m), 485 (w), 447 (vw), 403 (w), 369 (vw), 353 (vw), 330 (w-m). UV–vis spectral data (λ, nm; log ε) in CH₃CN: 216 (4.11), 263 (3.87); in CHCl₃: 263 (3.97). The same reaction conducted as above with the same quantities of reagents and identical reaction procedure confirmed the formation of comparable amounts of dhdpp (1.39 g) and dhdpp·2H₂O (43.5 mg). In a further attempt, under the same experimental conditions, pure dhdpp was obtained (935 mg, yield 40.0%). The mother liquors kept in the refrigerator for over 2 weeks led to the formation of a solid material which was separated by centrifugation, washed with ethanol, and brought to constant weight under vacuum (10⁻² mmHg, 262.8 mg). In the solid, partly composed of dhdpp·2H₂O, thin yellow needles were also found present (approximately 50% of the total amount of material), one of them isolated and examined by single-crystal X-ray analysis which established the needles to be dpp (Table S1; see the following Discussion section).

Synthesis of the Complexes [(dhdpp)MX₂]·xH₂O and Their Analogs [(dpp)MX₂]·xH₂O (M = Pt^{II}, Pd^{II}; X = Cl, OAc). [(dhdpp)PtCl₂]·5H₂O. This complex was previously prepared and formulated as [(dhdpp)PtCl₂]·H₂O·0.3CH₃OH.⁶ Following the reported procedure, the differently formulated complex, i.e., [(dhdpp)PtCl₂]·5H₂O, was obtained by us as follows: addition of dhdpp (28.2 mg, 0.119 mmol) to a solution of [(DMSO)₂PtCl₂] (50.4 mg, 0.119 mmol) in CH₃OH (10.0 mL) determines a rapid color change of the mixture from yellow to red. After 30 minutes, the formed brown crystalline material was separated by centrifugation, washed twice with CH₃OH, and brought to constant weight under vacuum (10⁻² mmHg, 44.0 mg, yield 73.6%). Calcd for [(dhdpp)PtCl₂]·5H₂O, C₁₄H₂₂Cl₂N₄O₅Pt: C, 28.39; H, 3.74; N, 9.46; Pt, 32.93%. Found: C, 28.14; H, 3.00; N, 9.00; Pt, 32.48%. IR (cm⁻¹): 3527 (sh), 3414 (w-m), 3068 (w), 3040 (w), 1594 (w), 1574 (vw), 1554 (vw), 1526 (vw), 1493 (vw), 1465 (m), 1412 (m), 1337 (w), 1282 (w), 1239 (w), 1155 (w), 1088 (vw), 1060 (vw), 1017 (m-s), 986 (w), 906 (w), 858 (vw), 798 (w), 774 (s), 744 (w-m), 697 (vw), 662 (vw), 638 (vw), 616 (w), 568 (w-m), 514 (vw), 478 (vw), 444 (w), 347 (sh)/335 (m) (ν_{Pt-Cl}). UV–vis spectral data (λ, nm (log ε)) in CH₃CN: 222, sh (4.06), 270 (5.97), 344 (3.56), 445 (3.50); in CHCl₃: 276 (3.95), 352 (3.51), 465 (3.56). ¹H NMR (300 MHz, CDCl₃): δ/ppm = 9.95 (d, J = 5.0 Hz, 1H, H₆); 8.49 (d, J = 4.7 Hz, 1H, H_{6'}); 8.10 (d, J = 7.8 Hz, 1H, H_{3'}); 7.98 (td, J = 1.7 Hz, 7.79 Hz, 1H, H_{4'}); 7.83 (td, J = 1.2 Hz, 7.92 Hz, 1H, H₄); 7.69 (td, J = 1.3 Hz, 5.86 Hz, 1H, H₅); 7.49 (m, 1H, H_{5'}); 6.86 (d, J = 8.1 Hz, 1H, H₃); 4.64 (t, J = 6.5 Hz, 7.45 Hz, 2H, H_a); 3.92 (t, J = 7.4 Hz, 7.21 Hz, 2H, H_b).

[(dpp)PtCl₂]·3H₂O. This complex, previously prepared and formulated as [(dpp)PtCl₂],^{3b,i} was obtained as follows: a suspension of (DMSO)₂PtCl₂ (72.1 mg, 0.171 mmol) in CH₃OH (7.5 mL) was added to dpp under stirring (40.0 mg, 0.171 mmol), and the mixture was heated at 60 °C for 2 h, with the color changing from the initial light yellow to red. After having been cooled to room temperature, the orange solid material was separated by centrifugation from the mother liquors, washed twice with CH₃OH, and brought to constant weight

under vacuum (50.0 mg, yield 52.7%). Calcd for [(dpp)PtCl₂]·3H₂O, C₁₄H₁₆Cl₂N₄O₃Pt: C, 30.34; H, 2.91; N, 10.11; Pt, 35.95%. Found: C, 30.57; H, 2.25; N, 9.70; Pt, 36.50%. IR (cm⁻¹): 3415 (w, broad), 3095 (vw), 3064 (vw), 3037 (m-w), 1639 (vw), 1594 (w), 1572 (w-m), 1554 (m), 1509 (vw), 1465 (w-m), 1438 (vww), 1429 (w), 1407 (s), 1394 (vs), 1313 (vww), 1286 (vww), 1259 (vww), 1236 (m), 1157 (s), 1121 (vw), 1090 (w), 1067 (w), 1058 (w), 1036 (w), 1018 (vw), 986 (w), 965 (vww), 884 (vww), 861 (m), 835 (vww), 807 (w), 786 (s), 754 (m-s), 741 (m-s), 665 (w), 651 (w), 620 (w), 585 (m), 554 (w), 482 (vw), 455 (w), 432 (vww), 406 (vw), 345 (m-s; ν_{Pt-Cl}), 325 (w). UV–vis spectral data (λ, nm; log ε) in CH₃CN: 275 (4.66), 339 (3.82), 405 (3.47); in CHCl₃: 278 (4.49), 337 (3.78), 424 (3.45). ¹H NMR (300 MHz, CDCl₃): δ/ppm = 10.05 (d, J = 3.1 Hz, 1H, H_a); 9.96 (d, J = 5.3 Hz, 1H, H₆); 8.83 (d, J = 3.1 Hz, 1H, H_b); 8.70 (d, J = 5.1 Hz; 1H, H_{6'}); 8.08 (td, J = 1.7 Hz, 7.70 Hz, 1H, H_{4'}); 7.99 (d, J = 7.9 Hz, 1H, H_{3'}); 7.80 (td, J = 1.5 Hz, 8.0 Hz, 1H, H₄); 7.58 (m, 2H, H₅, H_{5'}); 7.02 (d, J = 7.9, 1H, H₃).

[(dhdpp)PdCl₂]·2H₂O. The compound [(C₆H₅CN)₂PdCl₂] (71.4 mg, 0.186 mmol) was added to the solution obtained by dissolving dhdpp (44.0 mg, 0.186 mmol) in CH₃OH (2.0 mL) with a change of the initial orange color of the solution to mustard. Keeping the mixture under stirring for a few hours at room temperature led to the formation of a light-brown microcrystalline material which was separated by centrifugation, washed twice with CH₃OH, and brought to constant weight under vacuum (10⁻² mmHg, 61.40 mg, yield 79.7%). Calcd for [(dhdpp)PdCl₂]·2H₂O, C₁₄H₁₆Cl₂N₄O₂Pd: C, 37.40; H, 3.59; N, 12.46; Pd, 23.67%. Found: C, 37.93; H, 3.11; N, 12.60; Pd, 22.93%. IR (cm⁻¹): 3528 (w-m), 3410 (w-m), 3090 (vw), 3060 (w), 3038 (w-m), 2926 (vw), 2829 (vw), 1636 (vw), 1605 (w), 1585 (w), 1575 (m), 1540 (w-m), 1462 (m), 1425 (w-m), 1332 (m), 1282 (w-m), 1237 (m), 1155 (w-m), 1087 (w), 1063 (w), 1029 (w-m), 1016 (s), 988 (w-m), 906 (w), 858 (w), 803 (w-m), 776 (vs), 745 (m), 697 (vw), 656 (vw), 617 (w-m), 569 (m), 506 (vw), 435 (w-m), 411 (vw), 359 (w), 347 (m)/331 (m) (ν_{Pd-Cl}). UV–vis spectral data (λ, nm; log ε) in CH₃CN: 214 (4.61), 263 (4.19), 293, sh (3.97), 331 (3.67), 365 (3.54); in CHCl₃: 262, sh (4.24), 339 (3.64), 372 (3.55). ¹H NMR spectral data (300 MHz, CDCl₃): δ/ppm = 9.49 (d, J = 7.1 Hz, 1H, H₆); 8.48 (d, J = 4.8 Hz, 1H, H_{6'}); 8.11 (d, J = 7.8 Hz, 1H, H_{3'}); 7.97 (td, J = 1.6 Hz, 7.70 Hz, 1H, H_{4'}); 7.79 (td, J = 1.8 Hz, 7.00 Hz, 1H, H₄); 7.62 (td, J = 1.2 Hz, 7.00 Hz, 1H, H₅); 7.48 (m, 1H, H_{5'}); 6.84 (d, J = 8.0 Hz, 1H, H₃); 4.27 (t, J = 7.3 Hz, 7.40 Hz, 2H, H_a); 3.96 (t, J = 7.7, 6.90, 2H, H_b). It has been verified that the same complex was obtained with a procedure in which the reaction mixture was heated with stirring at 60 °C for 1 h (yield: 78.5%).

The same species in its hydrated form [(dhdpp)PdCl₂]·4H₂O was also prepared using dhdpp and PdCl₂ as reactants in the following procedure: PdCl₂ (25.3 mg, 0.135 mmol) was added to a solution of dhdpp (20.3 mg, 0.085 mmol) in CH₃CN (10 mL), and the mixture was kept under stirring at room temperature for 20 h. The light brown colored solid formed was separated by centrifugation from the mother liquors, washed twice with CH₃CN, and brought to constant weight under vacuum (15.9 mg, yield 45.2%). Calcd for [(dhdpp)PdCl₂]·4H₂O, C₁₄H₂₀Cl₂N₄O₄Pd: C, 34.62; H, 4.15; N, 11.54; Pd, 21.91%. Found: C, 34.91; H, 3.32; N, 11.20; Pd, 21.30%. ¹H NMR spectral resonance peaks for this species in CDCl₃ are found perfectly coincident with those already given for the sample prepared using [(C₆H₅CN)₂PdCl₂] as reactant (see above).

[(dpp)PdCl₂]·3H₂O. This complex, previously prepared and formulated as [(dpp)PdCl₂],^{3a,g} was obtained with a different procedure conducted here as follows: a brown suspension of PdCl₂ (44.6 mg, 0.252 mmol) and dpp (60.0 mg, 0.256 mmol) in CH₃OH (8.0 mL) was kept under stirring at room temperature for 20 h. The mustard colored solid formed was separated from the mother liquors by filtration, washed twice with CH₃OH, and brought to constant weight under vacuum (10⁻² mmHg, 60.5 mg, yield 51.6%). Calcd for [(dpp)PdCl₂]·3H₂O, C₁₄H₁₆Cl₂N₄O₃Pd: C, 36.11; H, 3.46; N, 12.03; Pd, 22.85%. Found: C, 35.72; H, 2.84; N, 11.70; Pd, 23.40%. IR (cm⁻¹): 3490 (m-w, broad), 3073 (w-m), 3046 (w-m), 1590 (m), 1554 (vw), 1509 (vww), 1460 (m-s), 1447 (vww), 1407 (vs), 1317

(vw), 1282 (vw), 1241 (m), 1161 (m-s), 1129 (vww), 1108 (vww), 1062 (m), 1031 (w-m), 1018 (w-m), 986 (vww), 973 (vww), 911 (vww), 897 (vww), 858 (w), 830 (vw), 807 (w), 799 (vw), 777 (s), 754 (w), 651 (w), 620 (vww), 598 (m-w), 585 (w), 549 (w), 473 (w), 442 (vw), 419 (vw), 350 (s; $\nu_{\text{Pd-Cl}}$), 307 (w), 286 (w). UV-vis spectral data (λ , nm; log ϵ) in CH_3CN : 209 (4.37), 276 (3.89), 327 (3.67); in CHCl_3 : 277 (4.15), 330 (3.77). ^1H NMR (300 MHz, CDCl_3): δ /ppm = 9.57 (d, J = 2.9 Hz, 1H, Ha); 9.53 (dd, J = 0.8 Hz, 5.8 Hz, 1H, H6); 8.89 (d, J = 2.9 Hz, 1H, Hb); 8.67 (dt, J = 1.7 Hz, 0.50 Hz, 4.6 Hz; 1H, H6'); 8.05 (m, 2H, H4', H3'); 7.74 (td, J = 1.6 Hz, 7.92 Hz, 1H, H4); 7.56 (m, 2H, H5, H5'); 7.02 (dd, J = 0.7 Hz, 8.2, 1H, H3).

Attempt of Synthesis of [(dhdpp)Pd(OAc)₂]. A solution of $\text{Pd}(\text{OAc})_2$ (41.8 mg, 0.186 mmol) in THF (4.0 mL) was added to a solution of dhdpp (44.0 mg, 0.186 mmol) in the same solvent (2.0 mL), and the purple-red solution was kept at room temperature for 90 minutes. The solid formed was separated by centrifugation, repeatedly washed with THF, and brought to constant weight under vacuum (10^{-2} mmHg, 58.0 mg, yield 56.6%). Calcd for [(dhdpp)Pd(OAc)₂] \cdot 5H₂O, C₁₈H₂₈N₄O₉Pd: C, 39.25; H, 5.12; N, 10.17; Pd, 19.32%. Found: C, 38.99; H, 4.59; N, 10.82; Pd, 19.69%. IR (cm⁻¹): 3410 (m), 3056 (vw), 1613 (s), 1586 (vs), 1460 (m), 1393 (s), 1314 (m), 1153 (w), 1015 (vw), 776 (w), 687 (w), 622 (vw), 583 (vw), 473 (vw). UV-vis spectral data (λ , nm; log ϵ) in CH_3CN : 270 (3.94), 323, sh (3.61); in CHCl_3 : 274 (4.34), 333, sh (3.78); in H_2O : 265 (4.51), 333, sh (3.72). As shown by the following NMR spectral data, the complex has been identified as a dpp derivative, and its correct formulation is [(dpp)Pd(OAc)₂] \cdot 5H₂O, also well supported by the above found elemental analyses (see the Discussion section below). ^1H NMR (300 MHz, CDCl_3): δ /ppm = 8.84 (d, J = 2.9 Hz, 1H, Ha); 8.69 (d, J = 4.1 Hz, 1H, H6); 8.52 (d, J = 2.9 Hz, 1H, Hb); 8.50 (d, J = 6.1 Hz, 1H, H6'); 8.05 (td, J = 1.7 Hz, 7.8 Hz, 1H, H4'); 7.94 (d, J = 7.7 Hz, 1H, H3'); 7.75 (m, 1H, H4); 7.59 (m, 1H, H5); 7.51 (m, 1H, H5'); 6.99 (d, J = 8.2 Hz, 1H, H3); 2.19, 2.18 (6H, 2CH₃).

[(dpp)Pd(OAc)₂] \cdot 2H₂O. This is a new Pd^{II}-dpp derivative directly prepared as follows: a solution of $\text{Pd}(\text{OAc})_2$ (48.1 mg, 0.214 mmol) in THF (4.0 mL) was added to a solution of dpp (49.0 mg, 0.209 mmol) in the same solvent (2.0 mL), and the resulting purple-red solution was kept at room temperature for 3 h. The solid formed was separated from the mother liquors by centrifugation, repeatedly washed with THF, and brought to constant weight under vacuum (10^{-2} mmHg, 59.3 mg, yield 57.3%). Calcd for [(dpp)Pd(OAc)₂] \cdot 2H₂O, C₁₈H₂₀N₄O₆Pd: C, 43.69; H, 4.07; N, 11.32; Pd, 21.51%. Found: C, 43.38; H, 3.91; N, 10.74; Pd, 20.87%. IR (cm⁻¹): 3425 (w-m), 3099 (vww), 3055 (vw), 2984 (vww), 2926 (vww), 1641 (vs), 1597 (s), 1564 (m), 1500 (vww), 1474 (w-m), 1406 (s), 1360 (s), 1312 (vs), 1298 (s), 1273 (m), 1161 (w), 1150 (w), 1074 (vw), 1061 (w), 1043 (w), 1007 (w), 993 (w), 912 (vw), 858 (vww), 837 (vww), 816 (vww), 789 (m), 773 (w), 754 (w). UV-vis spectral data (λ , nm; log ϵ) in CH_3CN : 270 (4.22), 325 (3.86), 527 (3.10); in CHCl_3 : 266, sh (4.18), 325 (3.95), 432 (3.23), 536 (3.15); in H_2O : 269 (4.23), 326 (3.93). ^1H NMR (300 MHz, CDCl_3): δ /ppm = 8.83 (d, J = 2.8 Hz, 1H, Ha); 8.68 (d, J = 4.1 Hz, 1H, H6); 8.52 (d, J = 2.9 Hz, 1H, Hb); 8.50 (d, J = 6.3 Hz, 1H, H6'); 8.04 (td, J = 1.8 Hz, 7.7 Hz, 1H, H4'); 7.93 (d, J = 7.8 Hz, 1H, H3'); 7.73 (m, 1H, H4); 7.58 (m, 1H, H5); 7.49 (m, 1H, H5'); 6.98 (d, J = 7.6 Hz, 1H, H3); 2.19, 2.18 (6H, 2CH₃).

[(CH₃)dhdpp]PdI₂[(I) \cdot 7H₂O]. The complex [(dhdpp)PdCl₂] \cdot 2H₂O (20.0 mg, 0.044 mmol) was suspended in CH_3CN (5.0 mL), and CH_3I was added (100.0 μL , molar ratio 1:33). The mixture was heated with stirring at 70 °C for 3 h, with the color of the suspension changing from brown to dark red. After having been cooled to room temperature, the mixture was kept in the refrigerator for 24 h. The solid present in the suspension was separated from the mother liquors by centrifugation, washed twice with CH_3CN , and brought to constant weight under vacuum (10^{-2} mmHg, 12.0 mg, yield 44.8%). Calcd for the formula [(CH₃)dhdpp]PdI₂[(I) \cdot 7H₂O, C₁₅H₂₉N₄I₃O₇Pd: C, 20.84; H, 3.38; N, 6.48; Pd, 12.31%. Found: 20.33; H, 3.12; N, 6.18; Pd, 12.90%. IR (cm⁻¹): 3600–3300 (broad, w-m) 3064 (w-m), 3051 (w-m), 2997 (w), 2961 (w), 2867 (w), 1581

(m), 1554 (vw), 1460 (s), 1425 (m-s), 1330 (s), 1286 (w), 1251 (w), 1233 (m), 1157 (m), 1085 (w), 1062 (w), 1031 (m-s), 1021 (m-s), 1004 (m), 866 (vw), 790 (w), 772 (vs), 746 (w), 728 (w), 651 (vw), 611 (vw), 562 (vw), 518 (w), 478 (w), 437 (vw), 419 (w), 345 (w-m), 317 (w-m). UV-vis spectral data (λ , nm; log ϵ) in CH_3CN : 208 sh (4.60), 247 (4.44). From the mother liquors kept in the refrigerator for a long time a small amount of small brown colored crystals was isolated of the complex of formula [(dpp)PdI₂], as was unequivocally established by single-crystal X-ray work (Table S1; see Discussion section below).

X-ray Crystallographic Measurements. Single crystal X-ray intensity data for all compounds were collected at room temperature on a Bruker SMART 1000 CCD diffractometer equipped with graphite monochromated Mo $K\alpha$ radiation (λ = 0.71073 Å). Data collection and reduction were carried out using the APEX2 and SAINT packages.^{11a} Multiscan absorption correction using the SADABS software^{11a} was applied to the intensity data. The structures were solved by direct methods using SHELXT^{11b} and refined with full-matrix least-squares on F^2 on all unique reflections using SHELXL-2018/3.^{11c} All the non-hydrogen atoms were refined anisotropically. The hydrogen atoms were placed geometrically and refined using a riding atom approximation, with C–H = 0.93–0.96 Å, and with $U_{\text{iso}}(\text{H}) = 1.2U_{\text{eq}}(\text{C})$ or $U_{\text{iso}}(\text{H}) = 1.5U_{\text{eq}}(\text{C})$ for methyl H atoms. In complex [(dpp)Pd(OAc)₂] a rotating model was used for the methyl groups, and ISOR restraints were applied. The very poor quality of the crystals of [(dpp)Pd(OAc)₂] available for data collection may account for the very high R_{int} and poor R factors obtained in the refinement.

Sequential ^1H NMR Analysis of dhdpp Conversion into dpp. A 5 mm NMR tube was charged with dhdpp (14 mg, 0.0592 mmol), $\text{Pd}(\text{OAc})_2$ (1.6 mg, 0.00713 mmol) (molar ratio 8.3:1), and THF- d_6 (0.60 mL), then flushed with nitrogen, and sealed with an NMR pressure cap. The mixture was shaken just before introduction into the NMR probe, thermostated at 24 °C. The sequence of spectra was obtained with 30 min time intervals or longer at advanced reaction stages. The spectra were analyzed by integration of the singlet signal at 8.62 ppm (dpp) with respect to the solvent signal at 1.74 ppm, taken as internal reference. Relative concentration of dhdpp and dpp can be obtained by integration of the signals at 8.16 ppm (d, J = 4.2 Hz) and at 8.62 ppm, respectively.

Other Physical Measurements. IR spectra were recorded on a Varian FT-IR 660 in the range 4000–250 cm⁻¹ (KBr pellets or nujol mulls between CsI disks). UV-vis solution spectra were recorded with a Varian Cary SE spectrometer using 1 cm quartz cuvettes. ^1H NMR spectra were recorded on a Bruker 300 AvanceII spectrometer operating at 300 MHz and referenced to the residual solvent signal (CHCl_3 , $\delta_{\text{H}} = 7.26$ ppm; CD_3CN , $\delta_{\text{H}} = 1.96$ ppm). X-ray Diffraction (XRD) patterns were obtained with a Philips PW 1729 diffractometer using $\text{CuK}\alpha$ (Ni-filtered) radiation in the 5–60° 2θ range (step size 0.02°; time per step 1.25 s). Elemental analyses for C, H, N, and S were provided by the “Servizio di Microanalisi” at the Department of Chemistry, Università Sapienza (Rome), using an EA 1110 CHNS-O instrument. The ICP-PLASMA Pd and Pt analyses were performed on a Varian Vista MPX CCD simultaneous ICP-OES. GC-MS analyses were obtained on an Agilent Technologies 6890N Network GC System equipped with a 5973 Network Mass Selective Detector.

DISCUSSION

As evidenced in the Introduction, the present project was planned as an investigation on the modes of bidentate chelation, either of the type “py-py” or “py-pyz”, present in the mononuclear complexes formed by 5,6-di-(2-pyridyl)-2,3-dihydropyrazine (dhdpp) formulated as [(dhdpp)MX₂] (M = Pd^{II}, Pt^{II}; X = Cl, OAc), having as a base of information what was previously reported on dpp and derivatives in a recent review.² During the development of this work, the tendency of dhdpp to undergo the already mentioned process dhdpp → dpp was accurately taken care of; as it will be shown, formation

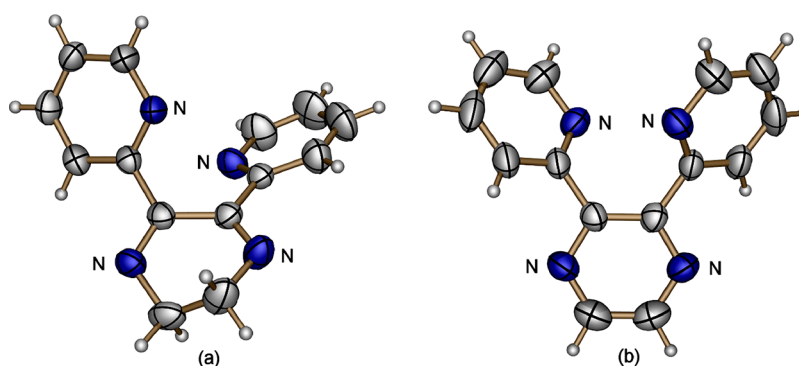


Figure 2. ORTEP view (50% probability ellipsoids) of (a) dhdpp and (b) dpp.

of dpp has been found to take place under a variety of experimental conditions.

Synthesis and Properties of 5,6-Di-(2-pyridyl)-2,3-dihydropyrazine (dhdpp). The synthesis of dhdpp, conducted as previously reported,⁷ led in our synthetic procedure to two different compounds, i.e., dhdpp and dhdpp·2H₂O. As established by previously reported X-ray work, duplicated by us (data in Table S1, Supporting Information) dhdpp shows (Figure 2a) a noncoplanar arrangement of the two pyridine rings, both of them also noncoplanar with the dihydropyrazine ring, this latter highly far from the full planarity present instead in the aromatic pyrazine ring of dpp (Figure 2b).¹² The dissimilar structural and electronic distribution present in the dihydropyrazine ring and the parent pyrazine ring was thought to determine in the first one an enhancement of its own N donor properties, the main object of research of the present work.

The IR spectra of dhdpp and dhdpp·2H₂O are shown in Figure 3 (region 3500–300 cm⁻¹). The spectrum of dhdpp (Figure 3A) is identical to that reported.¹⁰ The presence of H₂O in the spectrum of dhdpp·2H₂O (Figure 3B) is well evidenced by narrow intense peaks at 3312 cm⁻¹ (O–H

stretching) and 1648 cm⁻¹ (H₂O bending) suggesting a precise location of H₂O in the crystalline phase of the species. The X-ray powder spectra of the two species (Figure S2) reveal a high level of crystallinity. Comparison of the two spectra clearly indicates that they are not isomorphous. Attempts to obtain crystals for dhdpp·2H₂O suitable for single crystal X-ray work were not successful.

It is of great interest that in one synthetic procedure of dhdpp (Experimental Section), thin yellow crystalline needles were also formed in the mixture with a second component by long-standing of the mother liquors. One of the crystals was isolated and examined by single crystal X-ray work, which established the needles to be the compound dpp (Figure 2b; crystal data in Table S1; ¹H NMR spectrum in Figure S1B) evidently formed from dhdpp as a result of the dehydrogenation process dhdpp → dpp. The IR spectrum of the solid crystalline mixture (Figure S3) indicates that the second component is dhdpp·2H₂O, as clearly suggested by the two narrow peaks present at 3312 and 1648 cm⁻¹ due to H₂O (no attempts to separate the two species were made). From these data it has been possible to learn that formation of dpp from dhdpp can take place in the absence of a catalyst, as was instead the case for the above cited process determined by a palladium/charcoal catalyst.⁷

[(dhdpp)MCl₂]·xH₂O (M = Pt^{II}, Pd^{II}). Among the present dhdpp derivatives, the complex [(dhdpp)PtCl₂]·5H₂O is considered first since it is the only one having a previously reported analog useful for comparison and formulated as [(dhdpp)PtCl₂]·H₂O·0.3CH₃OH,⁶ our compound appositely similarly prepared although obtained with a different formulation, i.e., [(dhdpp)PtCl₂]·5H₂O (Experimental Section). The ¹H NMR spectrum in CDCl₃ of our complex (Figure 4) shows the presence of ten resonance peaks; eight of them are present in the region of the aromatic protons (6–10 ppm): four of which (3, 4, 5, 6) are assigned to the H atoms of the pyridine ring involved in the coordination to Pt^{II}, and the other four (3', 4', 5', 6') are attributable to the protons of the other pyridine ring. The two additional resonance peaks present in the region 3.8–4.8 ppm are assigned to the protons of the two CH₂ groups present in the dihydropyrazine ring of the complex. These spectral features perfectly coincide with those previously reported,⁶ thus definitely confirming for the complex [(dhdpp)PtCl₂] coordination of the type “py-pyz”. These results clearly indicate that despite the different formulation, the presence in the two species of solvent molecules does not affect the intimate structural environment in [(dhdpp)PtCl₂].

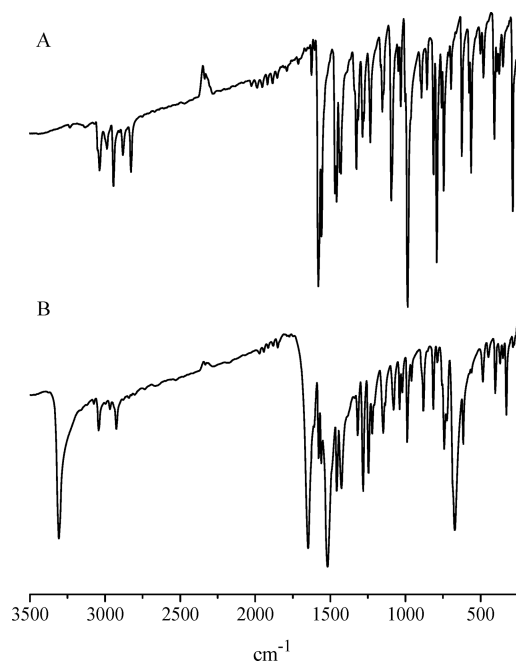


Figure 3. IR spectra of dhdpp (A) and dhdpp·2H₂O (B).

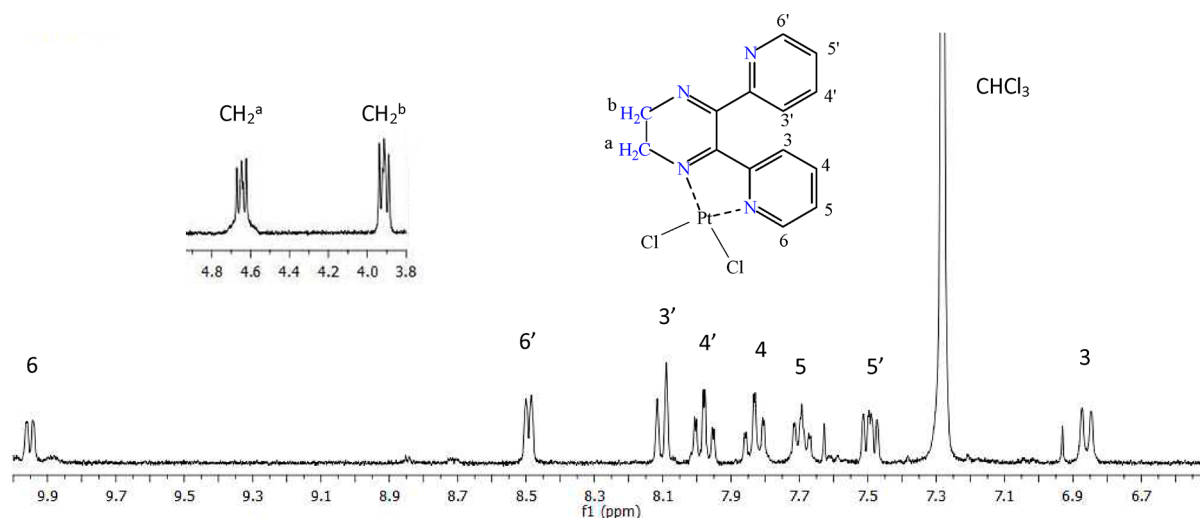


Figure 4. ^1H NMR spectrum in CDCl_3 of $[(\text{dhdpp})\text{PtCl}_2]\cdot 5\text{H}_2\text{O}$.

In a second test planned to examine the tendency of dhdpp to coordinate in a “py-pyz” fashion, samples of the Pd^{II} analog $[(\text{dhdpp})\text{PdCl}_2]\cdot 2\text{H}_2\text{O}$ were obtained using different reaction conditions in two distinct preparative procedures (Experimental Section, yields ca. 80%). Elemental analyses in both cases confirm for the complex the given formulation. The X-ray powder spectrum of the compound (Figure 5A) shows a high

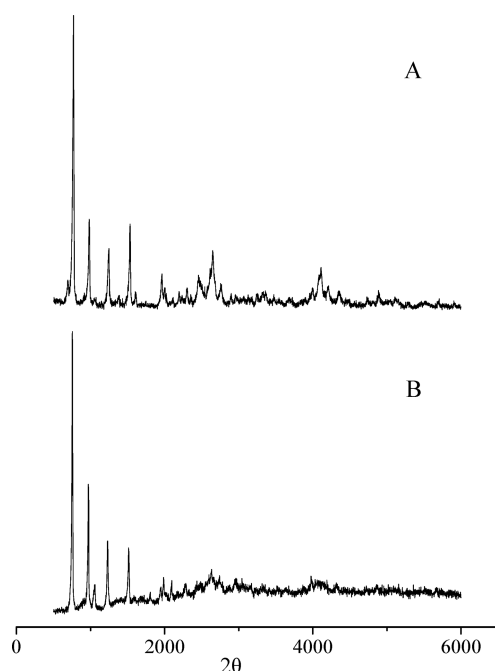


Figure 5. X-ray powder spectra of $[(\text{dhdpp})\text{PdCl}_2]\cdot 2\text{H}_2\text{O}$ (A) and $[(\text{dhdpp})\text{PtCl}_2]\cdot 5\text{H}_2\text{O}$ (B).

crystalline character. Comparison of the spectrum with that of the Pt^{II} analog (Figure 5B) indicates isomorphism between the two species. This result strongly suggests that the Pd^{II} complex also involves the metal center in a “py-pyz” mode of coordination.

The IR spectra of the Pd^{II} and Pt^{II} complexes are closely similar in all regions explored (Figure 6). The spectrum of the Pd^{II} species (Figure 6A) shows two distinct absorptions with

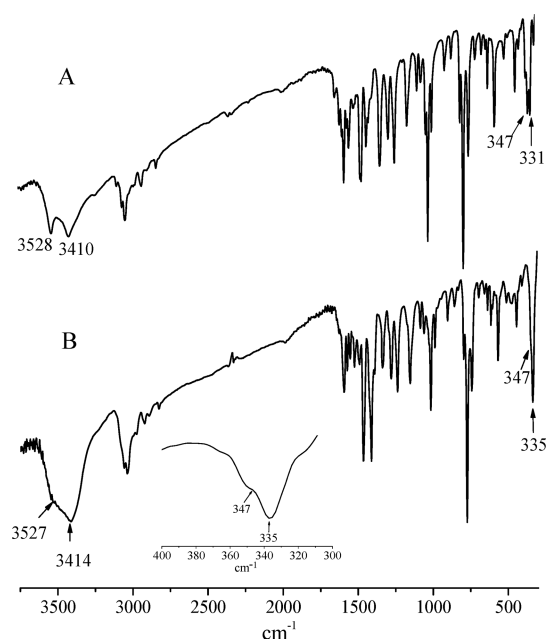


Figure 6. IR spectra of $[(\text{dhdpp})\text{PdCl}_2]\cdot 2\text{H}_2\text{O}$ (A) and $[(\text{dhdpp})\text{PtCl}_2]\cdot 5\text{H}_2\text{O}$ (B) in the range $3750\text{--}300\text{ cm}^{-1}$.

peaks at 3528 and 3410 cm^{-1} due to H_2O , peaks due to C–H bonds at ca. 3000 cm^{-1} , and, worth being noticed, a composed peak present at $347/331\text{ cm}^{-1}$ assigned as $\nu_{\text{Pd-Cl}}$ assignment encouraged by the absorption positioned at $340/335\text{ cm}^{-1}$ for the structurally characterized complex $[(\text{CN})_2(\text{dpp})\text{PdCl}_2]$.⁴

Similarly, the IR spectrum of the Pt^{II} species (Figure 6B) shows a broad band in the region $3600\text{--}3300\text{ cm}^{-1}$ with a peak at 3414 cm^{-1} and shoulder at 3527 cm^{-1} , positions practically coincident with those of the Pd^{II} analog, with broadening in the region caused most probably by the three additional disordered water molecules and peaks in the region at ca. 3000 cm^{-1} also assigned to the stretching of the C–H groups. Noteworthy, the observed narrow intense peaks at 347 (sh) and 335 cm^{-1} (Figure 6B, see inset) are assigned as $\nu_{\text{Pt-Cl}}$ in line with a similar assignment made for the absorption observed in an identical position for the complex of the known structure having the formula $[(\text{CN})_2\text{dpp}]\text{PtCl}_2$ ⁵ (Figure 1).

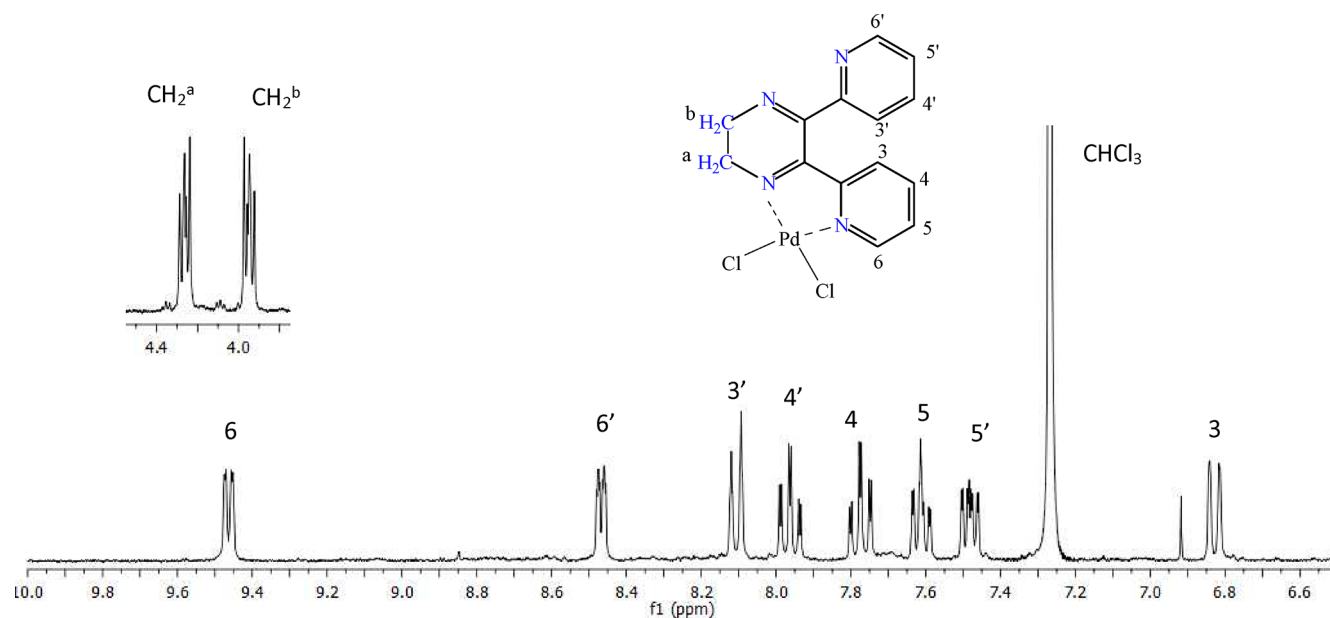


Figure 7. ^1H NMR spectrum in CDCl_3 of $[(\text{dhdpp})\text{PdCl}_2]\cdot 4\text{H}_2\text{O}$.

The established form of “py-pyz” coordination for the Pd^{II} and Pt^{II} complexes finds useful further support from the comparison of their ^1H NMR spectra. In fact, the ^1H NMR spectrum of the Pd^{II} species (Figure S4) shows main peak resonance positions exactly as for the Pt^{II} analog. However, owing to the presence of numerous low intensity resonance peaks due to small amounts of unknown species, the complex was also prepared under mild reaction conditions using PdCl_2 as the Pd^{II} reactant instead of $[(\text{C}_6\text{H}_5\text{CN})_2\text{PdCl}_2]$. The ^1H NMR spectrum of the new compound $[(\text{dhdpp})\text{PdCl}_2]\cdot 4\text{H}_2\text{O}$ (Figure 7) indicates the complete absence of impurities again confirming the presence of a “py-pyz” mode of coordination. It is also appropriate here to notice that the two different used reaction procedures (solvent, Pd^{II} reactant) lead to the same form of coordination, thus supporting the tendency of dhdpp to prefer the “py-pyz” coordination, similar to what was firmly established for the Pt^{II} analog.

$[(\text{dpp})\text{MCl}_2]\cdot 3\text{H}_2\text{O}$ ($\text{M} = \text{Pt}^{\text{II}}, \text{Pd}^{\text{II}}$). The two dpp analogs of the above Pd^{II} and Pt^{II} dhdpp complexes were obtained by us upon reaction of dpp in methanol with PdCl_2 or $(\text{DMSO})_2\text{PtCl}_2$, respectively, as the hydrated species of formula $[(\text{dpp})\text{MCl}_2]\cdot 3\text{H}_2\text{O}$ ($\text{M} = \text{Pt}^{\text{II}}, \text{Pd}^{\text{II}}$). The complexes parallel the respective nonsolvated species $[(\text{dpp})\text{MCl}_2]$ previously reported and structurally characterized.^{3a,d,h,i} Of these latter species, the Pt^{II} complex $[(\text{dpp})\text{PtCl}_2]$ is known only in its “py-pyz” mode of coordination,^{3h,i} whereas for the Pd^{II} analog both forms, i.e., “py-py” and “py-pyz”, were obtained “during the same preparative procedure”.^{3a,d} Both of our new hydrated species, obtained with methods different from those previously reported, show X-ray powder spectra (Figure S5) not indicative of an isostructural arrangement in the solid state. Indeed, their IR spectra in the region $3750\text{--}300\text{ cm}^{-1}$ are closely similar (Figure S6), both showing an intense narrow peak assigned as $\nu_{\text{M-Cl}}$ at 351 cm^{-1} for the Pd^{II} species and at 345 cm^{-1} for the Pt^{II} analog. Great help as to the type of metal-to-ligand coordination present in our two complexes $[(\text{dpp})\text{MCl}_2]\cdot 3\text{H}_2\text{O}$ is provided by their ^1H NMR spectra. The general common features of the spectra (Figure S7) unequivocally indicate for both complexes the “py-pyz” mode

of coordination. These results inform that using our synthetic procedure the observed “py-pyz” mode of coordination duplicates for both species the one already known for the nonhydrated parent species.^{3a,d,h,i}

Attempt of the Synthesis of a dhdpp Complex with $\text{Pd}(\text{OAc})_2$. In our third attempt to verify the tendency of dhdpp to give a “py-pyz” mode of coordination, the isolated new species formed from the reaction of dhdpp with $\text{Pd}(\text{OAc})_2$ is reproducibly obtained in THF under mild reaction conditions (Experimental Section). The amorphous character of the isolated material is clearly shown by its X-ray powder spectrum (Figure S8). Elemental analyses are in agreement for a compound having the formula $[(\text{dhdpp})\text{Pd}(\text{OAc})_2]\cdot 5\text{H}_2\text{O}$. The IR spectrum (Figure 8) is characterized

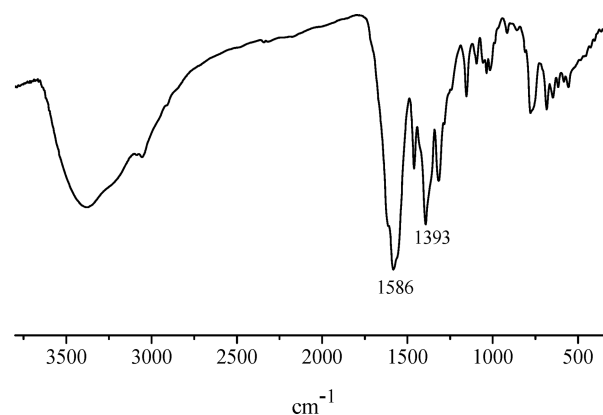


Figure 8. IR spectrum of the expected $[(\text{dhdpp})\text{Pd}(\text{OAc})_2]\cdot 5\text{H}_2\text{O}$.

by the presence of a broad intense absorption with maximum at ca. 3500 cm^{-1} due to the O–H stretching of H_2O and of two intense peaks at 1586 (covering also the O–H bending) and 1393 cm^{-1} assigned, respectively, to the stretching vibrations $\nu_{\text{C=O}}$ and $\nu_{\text{C-O}}$, close to those found for $\text{Pd}(\text{OAc})_2$ at 1603 cm^{-1} ($\nu_{\text{C=O}}$) and 1427 cm^{-1} ($\nu_{\text{C-O}}$).

The ^1H NMR spectrum of the compound (Figure 9) shows complete absence of the resonance peaks in the $3.8\text{--}4.2$ ppm

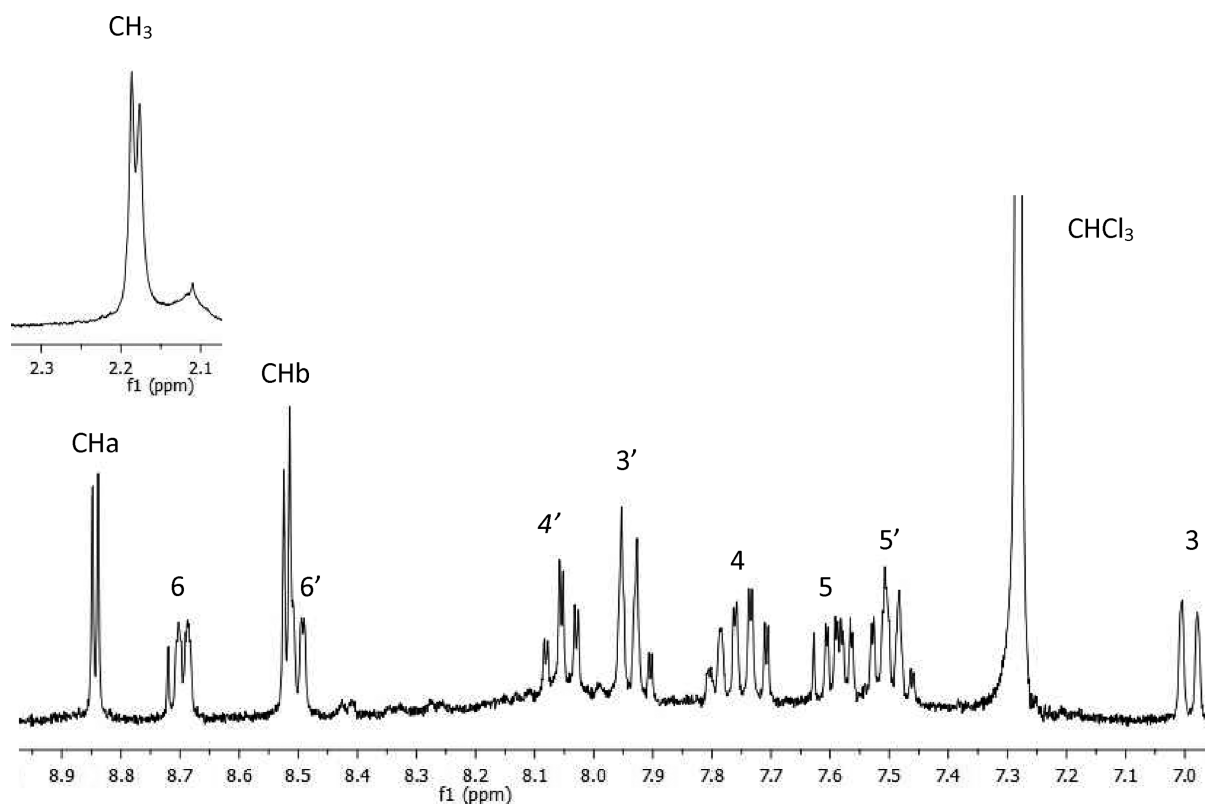


Figure 9. ^1H NMR spectrum in CDCl_3 of the synthesized complex formulated as $[(\text{dpp})\text{Pd}(\text{OAc})_2]\cdot 5\text{H}_2\text{O}$.

region expected for the H atoms of the two CH_2 groups of the dhdp ligand. In addition, the region of the aromatic hydrogen atoms (6.7–9.0 ppm), plausibly interpretable as due to the presence of the “py-pyz” mode of coordination, is also accompanied by the presence of two resonance peaks due to the hydrogen atoms of a pyrazine ring (CHa, CHb in Figure 9).

The inset shows two resonance peaks at 2.19 and 2.18 ppm assigned to the CH_3 groups present in the two OAc fragments. The observed NMR spectral features clearly suggest the hypothesis that a dhdp \rightarrow dpp process might have taken place. For further support of this, the dpp analog was appositely synthesized and obtained in the form of a bis-hydrated species of formula $[(\text{dpp})\text{Pd}(\text{OAc})_2]\cdot 2\text{H}_2\text{O}$ (see the Experimental Section). The ^1H NMR spectrum of a sample of this dpp species (Figure S9) coincides perfectly with that of the supposed pentahydrated dhdp derivative (Figure 9), for which the exact formulation is therefore $[(\text{dpp})\text{Pd}(\text{OAc})_2]\cdot 5\text{H}_2\text{O}$ (irrelevant in the two species the different presence of water). X-ray analysis of single crystals of the complex isolated from the mother liquors in its nonsolvated form illustrates the structural arrangement of the entire molecule (Figure 10).

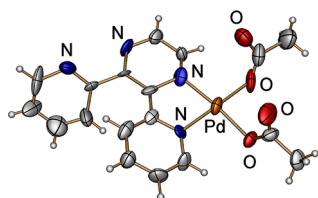


Figure 10. Molecular structure of $[(\text{dpp})\text{Pd}(\text{OAc})_2]$ with displacement ellipsoids drawn at the 50% probability level.

Crystal data are listed in Table S1; selected bond lengths and angles are given in Table S2. These results indicate that during the synthetic procedure of the planned dhdp derivative the ligand has been integrally changed to dpp. These findings are different from those exposed above in the case of dpp formed from dhdp only in low yield.

In the attempt to gain further insight into the transformation dhdp \rightarrow dpp, and in particular to understand if the process is catalytic in metal complex, the reaction of dhdp with $\text{Pd}(\text{OAc})_2$ in $\text{THF}-d_8$ has been followed *in situ* by ^1H NMR spectroscopy, at 24 $^\circ\text{C}$. The spectrum obtained immediately after mixing reveals the presence of a singlet signal at 8.62 ppm, which, along with the other signals, is unequivocally attributable to the C–H hydrogens of the pyrazine ring. In the course of the reaction, additional signals uncertainly attributable to $[(\text{dpp})\text{Pd}(\text{OAc})_2]$ become well distinguishable in the aromatic region. The spectrum taken after 5 minutes and the last one taken when the intensity of the singlet signal of dpp did not increase further (4 days) are shown in Figure 11A,B. A sequence of four spectra including two of them taken at intermediate times is shown in Figure S10. At the last registration (Figure 11B), the GC-MS analysis of the organic components in the reaction mixture indicated 3% and 97 mol % of dhdp and dpp, respectively, clearly indicating (Figure S11) that the dehydrogenation process proceeds with $\text{Pd}(\text{OAc})_2$ behaving as a catalyst.

A plot of the percent conversion of dhdp into dpp vs time (Figure 12) clearly identifies one rapid exponential phase (inset) followed by a slower zero-order phase.

The initial rapid conversion dhdp \rightarrow dpp can be attributed to the presence of $\text{Pd}(\text{OAc})_2$ in catalytic amounts, thus resulting in the reaction of dhdp proceeding under pseudo-first-order conditions. As the reaction develops further and

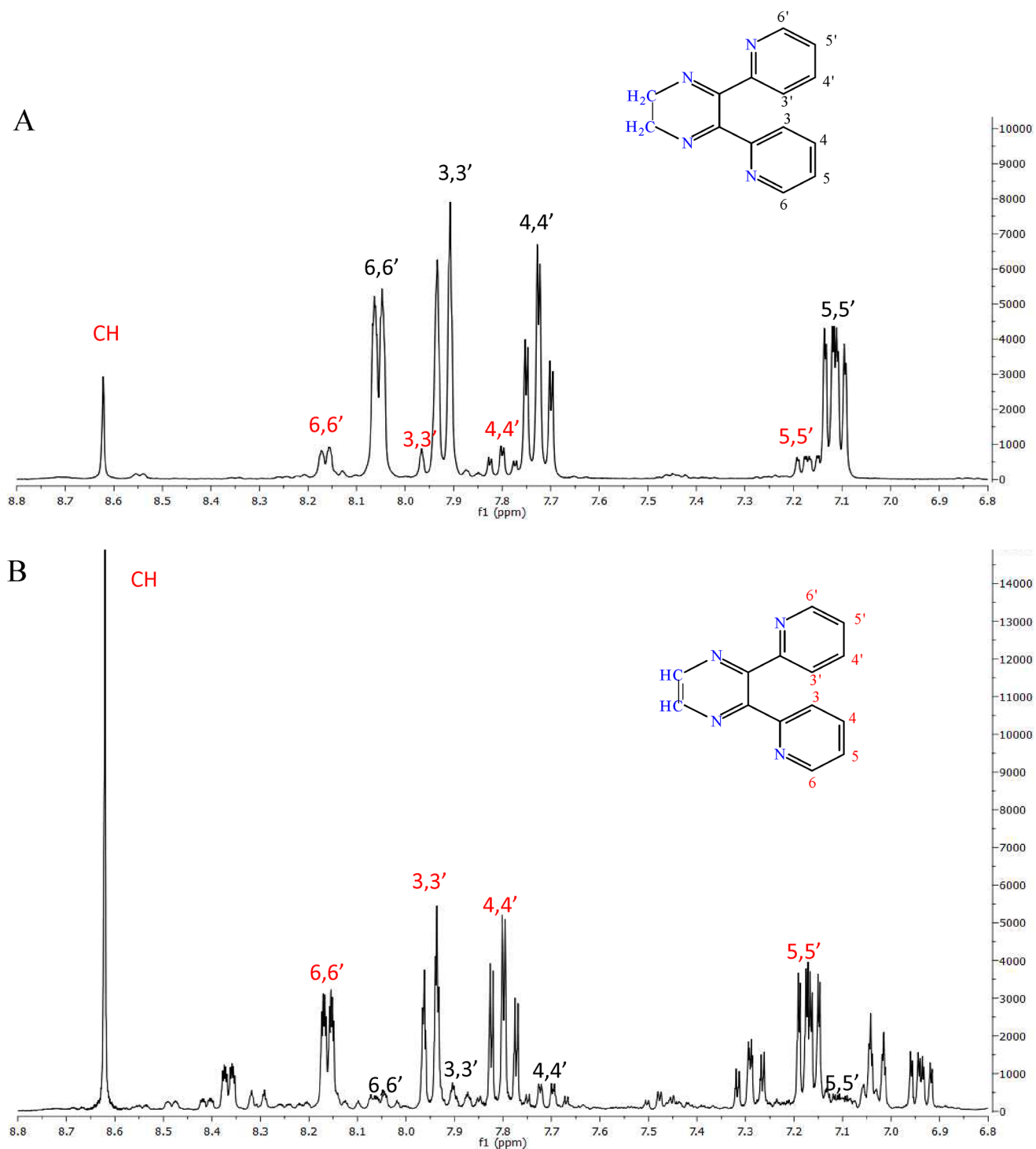


Figure 11. ^1H NMR (300 MHz, $\text{THF-}d_6$, 24 $^\circ\text{C}$) spectral evolution of dhdpp in the presence of $\text{Pd}(\text{OAc})_2$ (molar ratio 8.3:1): A) initial spectrum (5 min) and B) final spectrum (93 h).

$\text{Pd}(\text{OAc})_2$ is sequestered in the complex with dpp, as observed in solution as well as by separation of precipitate, the rate only depends on a slower rate-determining step not involving dhdpp, presumably the generation of an active palladium acetate species. A complex mixture of molecular complexes can be envisaged in solution during the course of the reaction, among which are dimeric palladium acetate, 1:1 adducts $\text{Pd}(\text{OAc})_2(\text{L})$ of either dhdpp or dpp, and also, due to the molar excess of the nitrogen ligands, 1:2 adducts $\text{Pd}(\text{OAc})_2(\text{L})_2$ with L as monodentate N-donors.¹³ Low-

coordination palladium species, hence prone to interaction with dhdpp, should then arise from reversible ligand dissociation processes. Among these is release of one ligand from Pd by solvent exchange or a switch of the coordination mode of dpp from bidentate to monodentate, which is possible due to the intrinsic hemilabile character of the N,N' ligand.¹⁴ Such a Pd–N bond-breaking step,¹⁵ if slower than the overall dehydrogenation reaction, would also be rate determining and thus account for the dominant zero-order phase shown in the graph of Figure 12.¹⁶ Although the details of the mechanism by

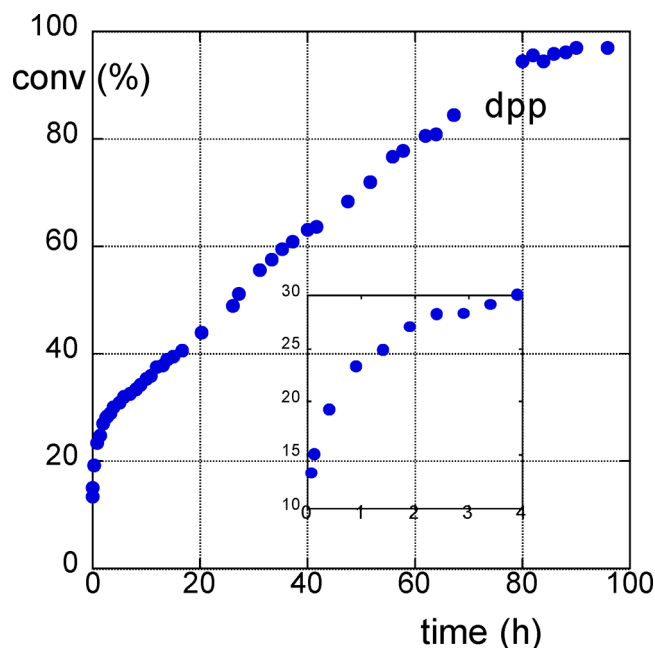


Figure 12. Percent formation of dpp vs time for the reaction of dhdp (14 mg, 0.099 mol L⁻¹) with Pd(OAc)₂ (1.6 mg, 12 mol %) in THF-d₈ (0.60 mL), as followed by ¹H NMR spectroscopy (24 °C).

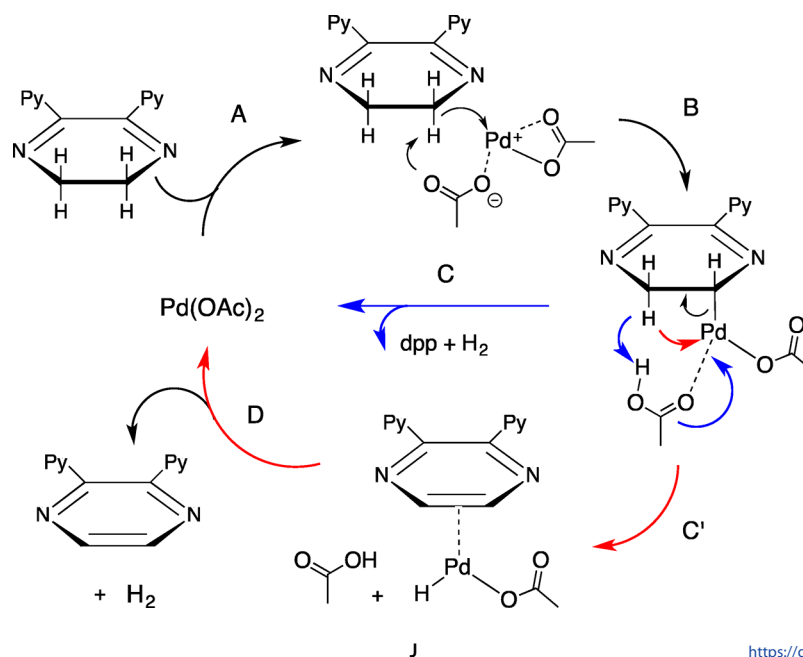
which palladium acetate catalyzes the dehydrogenation of the dhdp ligand should require further investigation, at present a catalytic cycle of the reaction can be envisaged as outlined in Scheme 1, based on typical organometallic palladium chemistry: *i*) hydrogen abstraction from a C(sp³)-H bond by the acetate ligand with C-Pd bond formation (step B) and *ii*) β-hydrogen elimination to form the double bond (steps C). With regard to step B, there are several examples of carboxylate-assisted palladium-catalyzed direct C(sp³)-H functionalization,¹⁷ also for C-H bonds in α to a nitrogen atom.¹⁸ The different outcome of the stoichiometric reaction between dhdp and PdCl₂, giving rise to [(dhdp)PdCl₂].4H₂O, discloses unambiguously the key role played by the

acetate counteranion in the dhdp → dpp transformation. Palladium acetate or palladium complexes in the presence of carboxylate salts are commonly used as dehydrogenation catalysts.¹⁹ Although harsh conditions and stoichiometric amounts of terminal oxidants are required, recent developments include milder conditions in a simple aerobic environment or even without oxidants.²⁰ What is rather peculiar in the experiment described here and worth pointing out is that dehydrogenation of dhdp initiated by Pd(OAc)₂ does proceed with high conversion and selectivity even in the presence of bidentate and strongly coordinating donor sites in the substrate, conditions believed to be incompatible with Pd^{II} catalyzed oxidation methods.^{20b}

[[{(CH₃)dhdp}PdI₂](I)·7H₂O. [(dhdp)PdCl₂], proved above to imply “py-pyz” coordination, was made to react with CH₃I under drastic reaction conditions intentionally promoting quaternization of the N atom of the pyridine ring not involved in the coordination to Pd^{II} and the predictable concomitant change PdCl₂ → PdI₂. Formation of the isolated fully iodinated species formulated on the basis of elemental analysis as a salt-like species of formula [[{(CH₃)dhdp}PdI₂](I)·7H₂O was expected, as the pyridine ring as such, not involved in the coordination to PdCl₂, could easily undergo quaternization of the N atom. This type of process is substantiated by the fact that in the case of the somehow related unmetallated 2,3-dicyano-5,6-di(2-pyridyl)-1,4-pyrazine, [(CN)₂Py₂Pyz], carrying two vicinal pyridine rings, contact with CH₃I in DMF under very mild reaction conditions (4 days at room temperature) leads to the formation of the related salt-like species [(CN)₂Py(2-Mepy)Pyz](I) (only one pyridine atom quaternized), of which the structure was elucidated by X-ray work.²¹

The stable-to-air hydrated salt-like species, formulated as [[{(CH₃)dhdp}PdI₂](I)·7H₂O in good agreement with elemental analyses, although explored by IR and UV-visible spectra, needs further studies for its characterization in terms of physicochemical properties and structural features. Deserving mention here is that during the examined reaction of [(dhdp)PdCl₂] with CH₃I a small amount of brown colored

Scheme 1. Suggested Catalytic Cycle for Dehydrogenation of dhdp by Pd(OAc)₂



crystals was isolated from the mother liquors kept in the refrigerator for a long time (see the [Experimental Section](#)). Crystallographic work identified the species as $[(\text{dpp})\text{PdI}_2]$ (Figure 13, crystal data in [Table S1](#)), a compound previously

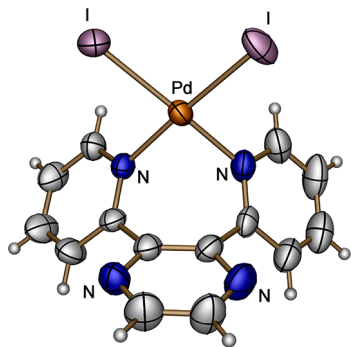


Figure 13. ORTEP view (50% probability ellipsoids) of the complex $[(\text{dpp})\text{PdI}_2]$.

reported^{3c} and showing the “py-py” mode of coordination. A tentative explanation of the formation of this species from the dhdp complex $[(\text{dhdp})\text{PdCl}_2]$ leads to suggest that dpp, once formed during the reaction, induces in the temporarily formed new species $[(\text{dpp})\text{PdCl}_2]$ an immediate change of the type of coordination from “py-pyz” to “py-py” with concomitant conversion of PdCl_2 to PdI_2 , this evidently preventing quaternization of even only one pyridine N atom by CH_3I . The overall process leading to formation of $[(\text{dpp})\text{PdI}_2]$ is a third established example in the present work of a $\text{dhdp} \rightarrow \text{dpp}$ process, with all three cases examined occurring in different chemical events. Incidentally, the conversion of $\text{PdCl}_2 \rightarrow \text{PdI}_2$ in $[(\text{dpp})\text{PdI}_2]$ supports that the same change has taken place leading to the formation of the above fully iodinated salt-like species.

CONCLUSIONS

In the present work the multiple N donor ligand 2,3-di-(2-pyridyl)-5,6-dihydropyrazine (dhdp) has been also isolated and characterized as a bis-hydrated derivative, $\text{dhdp} \cdot 2\text{H}_2\text{O}$. Unexpectedly, crystallization of dhdp occasionally allowed isolation from the mother liquors of a low amount of crystals proved by X-ray analysis to be the related dehydrogenated species 2,3-di-(2-pyridyl)-1,4-pyrazine (dpp) formed in the direct dehydrogenation process $\text{dhdp} \rightarrow \text{dpp}$. Central work was directed to deeply explore and define the type of coordination between the ligand dhdp and the metal center in the complexes of formula $[(\text{dhdp})\text{MCl}_2]$ (Pt^{II} , Pd^{II}). It has been firmly established, by X-ray powder, IR and ^1H NMR spectral data, that a “py-pyz” mode of coordination is favored with respect to the fairly equilibrated presence of “py-py” and “py-pyz” in the dpp analogs previously published and also studied in the present work. In our further attempt directed to support the tendency to coordinate in a “py-pyz” fashion, dhdp has been studied in its reaction with $\text{Pd}(\text{OAc})_2$. It has been observed that, during the course of the reaction, dhdp undergoes a change to dpp, the overall process leading to formation of the complex $[(\text{dpp})\text{Pd}(\text{OAc})_2]$, as established by ^1H NMR spectral data and crystallographic work. An additional detailed NMR investigation also definitely indicates that $\text{Pd}(\text{OAc})_2$ plays the role of catalyst in the observed $\text{dhdp} \rightarrow \text{dpp}$ conversion. This remarkable result introduces the

interesting further aspect of this work, i.e., the repeatedly verified tendency of dhdp, either in the absence or in the presence of a catalyst, to release hydrogen and form dpp under a variety of experimental conditions. As a further interesting related result, it has been proved that also in the synthetic work leading to the salt-like species $[(\text{CH}_3)\text{dhdp}]\text{PdI}_2(\text{I})$, a collateral process takes place in which once more dpp is formed from dhdp giving rise to the complex $[(\text{dpp})\text{PdI}_2]$, the structure of which has been elucidated by single-crystal X-ray work. These results clearly indicate that careful analysis is required when dealing with experimental work involving dhdp. Further extensive work is needed to enlarge the knowledge of the coordination chemistry of dhdp in mono-, di-, and multinuclear complexes.

ASSOCIATED CONTENT

Supporting Information

The Supporting Information is available free of charge at <https://pubs.acs.org/doi/10.1021/acs.inorgchem.0c00699>.

^1H NMR spectra of dhdp, dpp, $[(\text{dhdp})\text{PdCl}_2] \cdot 5\text{H}_2\text{O}$, $[(\text{dpp})\text{PdCl}_2] \cdot 3\text{H}_2\text{O}$, $[(\text{dpp})\text{PtCl}_2] \cdot 3\text{H}_2\text{O}$, and $[(\text{dpp})\text{Pd}(\text{OAc})_2] \cdot 2\text{H}_2\text{O}$; X-ray powder spectra of dhdp, $\text{dhdp} \cdot 2\text{H}_2\text{O}$, $[(\text{dpp})\text{PdCl}_2] \cdot 3\text{H}_2\text{O}$, $[(\text{dpp})\text{PtCl}_2] \cdot 3\text{H}_2\text{O}$, and $[(\text{dhdp})\text{Pd}(\text{OAc})_2] \cdot 5\text{H}_2\text{O}$; IR spectra of IR spectra of dpp in mixture with $\text{dhdp} \cdot 2\text{H}_2\text{O}$, $[(\text{dpp})\text{PdCl}_2] \cdot 3\text{H}_2\text{O}$, and $[(\text{dpp})\text{PtCl}_2] \cdot 3\text{H}_2\text{O}$; GC-MS analysis of the reaction between dhdp and $\text{Pd}(\text{OAc})_2$ (corresponding to final spectrum of [Figure 11B](#)); and tables reporting crystallographic and structural refinement data of dpp, dhdp, $[(\text{dpp})\text{Pd}(\text{OAc})_2]$, and $[(\text{dpp})\text{PdI}_2]$ and selected bond lengths and angles of $[(\text{dpp})\text{Pd}(\text{OAc})_2]$ and $[(\text{dpp})\text{PdI}_2]$ (PDF)

Accession Codes

CCDC 1958377–1958380 contain the supplementary crystallographic data for this paper. These data can be obtained free of charge via www.ccdc.cam.ac.uk/data_request/cif, or by emailing data_request@ccdc.cam.ac.uk, or by contacting The Cambridge Crystallographic Data Centre, 12 Union Road, Cambridge CB2 1EZ, UK; fax: +44 1223 336033.

AUTHOR INFORMATION

Corresponding Authors

Maria Pia Donzello – Dipartimento di Chimica, Università di Roma Sapienza, 00185 Roma, Italy; orcid.org/0000-0001-9084-0369; Email: mariapia.donzello@uniroma1.it

Mauro Bassetti – Dipartimento di Chimica, Università di Roma Sapienza, 00185 Roma, Italy; CNR - Istituto per i Sistemi Biologici, Sede di Roma - Meccanismi di Reazione, 00185 Roma, Italy; orcid.org/0000-0002-8163-3234; Email: mauro.bassetti@uniroma1.it

Corrado Rizzoli – Dipartimento di Scienze Chimiche, della Vita e della Sostenibilità Ambientale, Università di Parma, I-43124 Parma, Italy; orcid.org/0000-0002-4841-6123; Email: corrado.rizzoli@unipr.it

Claudio Ercolani – Dipartimento di Chimica, Università di Roma Sapienza, 00185 Roma, Italy; Email: claudio.ercolani@uniroma1.it

Authors

Edoardo Raciti – Dipartimento di Chimica, Università di Roma Sapienza, 00185 Roma, Italy

Elisa Viola – Dipartimento di Chimica, Università di Roma Sapienza, 00185 Roma, Italy

Ida Pettiti – Dipartimento di Chimica, Università di Roma Sapienza, 00185 Roma, Italy

Noemi Bellucci – Dipartimento di Chimica, Università di Roma Sapienza, 00185 Roma, Italy

Complete contact information is available at:

<https://pubs.acs.org/10.1021/acs.inorgchem.0c00699>

Notes

The authors declare no competing financial interest.

ACKNOWLEDGMENTS

Financial support by the University of Rome La Sapienza (Progetto di Ricerca - Anno 2017 – RM11715C819222B8) and by CNR-DISBA project NutrAge (7022) is gratefully acknowledged. M.P.D. is grateful to the Consorzio Interuniversitario di Ricerca in Chimica dei Metalli nei Sistemi Biologici (CIRCMSB) for scientific support.

REFERENCES

- (1) Clayden, J.; Greeves, N.; Warren, S. *Organic Chemistry*, 2nd ed.; Oxford University Press: 2012.
- (2) Floris, B.; Donzello, M. P.; Ercolani, C.; Viola, E. The chameleon-like coordinating ability of 2,3-di(pyridyl)pyrazine-type ligands. *Coord. Chem. Rev.* **2017**, *347*, 115–140.
- (3) (a) Ha, K. Dichlorido(2,3-di-2-pyridylpyrazine- κ^2N^2,N^3)-palladium(II). *Acta Cryst.* **2011**, *E67*, No. m1615. (b) Ha, K. Dibromido(2,3-di-2-pyridylpyrazine- κ^2N^2,N^3)palladium(II). *Acta Cryst.* **2011**, *E67*, No. m1896. (c) Ha, K. (2,3-Di-2-pyridylpyrazine- κ^2N^2,N^3)diiodidopalladium(II). *Acta Cryst.* **2011**, *E67*, No. m1626. (d) Ha, K. Dibromido(2,3-di-2-pyridylpyrazine- κ^2N^2,N^3)platinum(II). *Acta Cryst.* **2011**, *E67*, 1307. (e) Ha, K. (2,3-Di-2-pyridylpyrazine- κ^2N^2,N^3)diiodidoplatinum(II). *Acta Cryst.* **2012**, *E68*, No. m834. (f) Ha, K. (2,3-Di-2-pyridylpyrazine- κ^2N^2,N^3)bis(thiocyanato- η^5)palladium(II). *Acta Cryst.* **2012**, *E68*, No. m144. (g) Ha, K. Dichlorido(2,3-di-2-pyridylpyrazine- κ^2N^2,N^3)palladium(II). *Acta Cryst.* **2011**, *E67*, No. m1634. (h) Ng, Y.-Y.; Che, C.-M. Structure and spectroscopic properties of the Pt(dpp) X_2 (dpp = 2,3-bis(2-pyridyl)pyrazine)building blocks and the photophysical properties of heterometallic M-dpp-Pt supermolecules (M = Ru, Re, Pt). *New J. Chem.* **1996**, *20*, 781–789. (i) Ha, K. Dichlorido(2,3-di-2-pyridylpyrazine- κ^2N^2,N^3)platinum(II). *Acta Cryst.* **2011**, *E67*, No. m1454. (j) Ha, K. Dibromido(2,3-di-2-pyridylpyrazine- κ^2N^2,N^3)platinum(II). *Acta Cryst.* **2011**, *E67*, No. m1230. (k) Ferreira, A. D. Q.; Bino, A.; Gibson, D. Novel carboplatin analogs containing flexible and potentially intercalating ligands: preparation and X-ray crystal structures of di-2-pyridyl ketone cyclobutanedicarboxylate platinum (II) and of 2,3-bis(2-pyridyl) pyrazine cyclobutane dicarboxylate platinum (II). *Inorg. Chim. Acta* **1997**, *265*, 155–161. (l) Kennedy, F.; Shavaleev, N. M.; Koullourou, T.; Bell, Z. R.; Jeffery, J. C.; Faulkner, S.; Ward, M. D. Sensitized near-infrared luminescence from lanthanide(III) centres using Re(I) and Pt(II) diimine complexes as energy donors in d-f dinuclear complexes based on 2,3-bis(2-pyridyl)pyrazine. *Dalton Trans.* **2007**, 1492–1499.
- (4) Donzello, M. P.; Viola, E.; Cai, X.; Mannina, L.; Rizzoli, C.; Ricciardi, G.; Ercolani, C.; Kadish, K. M.; Rosa, A. Tetra-2,3-pyrazinoporphyrazines with externally appended pyridine rings. 5. Synthesis, physicochemical and theoretical studies of a novel pentanuclear palladium(II) complex and related mononuclear species. *Inorg. Chem.* **2008**, *47*, 3903–3919.
- (5) Cai, X.; Donzello, M. P.; Viola, E.; Rizzoli, C.; Ercolani, C.; Kadish, K. M. Structural, UV-Visible, and Electrochemical Studies on 2,3-Dicyano-5,6-di-2-pyridylpyrazine, [(CN) $_2$ Py $_2$ Pyz], Related Species and Its Complexes [(CN) $_2$ Py $_2$ PyzMCl $_2$] (M = Pt^{II}, Pd^{II}). *Inorg. Chem.* **2009**, *48*, 7086–7098.
- (6) Granifo, J.; Vargas, M. E.; Rocha, H.; Garland, M. T.; Baggio, R. Structural and coordinating properties of platinum(II) chloride complexes with polypyridyl ligands. Single crystal X-ray structure of [Pt(ddpq)Cl $_2$] \cdot H $_2$ O (ddpq = 6,7-dimethyl-2,3-di(2-pyridyl)-quinoxaline). *Inorg. Chim. Acta* **2001**, *321*, 209–214.
- (7) Goodwin, H. A.; Lions, F. Tridentate chelate compounds. II. *J. Am. Chem. Soc.* **1959**, *81*, 6415–6422.
- (8) Price, J. H.; Williamson, R. F.; Schramm, R. F.; Wayland, B. B. Palladium(II) and platinum(II) alkyl sulfoxide complexes. Examples of sulfur-bonded, mixed sulfur- and oxygen-bonded, and totally oxygen-bonded complexes. *Inorg. Chem.* **1972**, *11*, 1280–1284.
- (9) Kharasch, M. S.; Seyler, R. C.; Mayo, F. R. Coordination Compounds of Palladous Chloride. *J. Am. Chem. Soc.* **1938**, *60*, 882–884.
- (10) Posel, M.; Stoeckli-Evans, H. *IUCrData* **2016**, *1*, No. x161467.
- (11) (a) Bruker APEX2, SAINT and SADABS; Bruker AXS, Inc.: Madison, Wisconsin, USA, 2008. (b) Sheldrick, G. M. SHELXT - Integrated space-group and crystal-structure determination. *Acta Crystallogr., Sect. A: Found. Adv.* **2015**, *A71*, 3–8. (c) Sheldrick, G. M. Crystal structure refinement with SHELXL. *Acta Crystallogr., Sect. C: Struct. Chem.* **2015**, *C71*, 3–8.
- (12) Huang, N.-T.; Pennington, W. T.; Pedersen, J. D. Structure of 2,3-bis(2-pyridyl)pyrazine. *Acta Crystallogr., Sect. C: Cryst. Struct. Commun.* **1991**, *47*, 2011–2012.
- (13) Cook, A. K.; Sanford, M. S. Mechanism of the Palladium-Catalyzed Arene C-H Acetoxylation: A Comparison of Catalysts and Ligand Effects. *J. Am. Chem. Soc.* **2015**, *137*, 3109–3118.
- (14) (a) Slone, C. S.; Weinberger, D. A.; Mirkin, C. A. The Transition Metal Coordination Chemistry of Hemilabile Ligands. In *Progress in Inorganic Chemistry*; Karlin, K. D., Ed.; John Wiley & Sons: New York, 1999; Vol. 48, pp 233–350, DOI: 10.1002/9780470166499.ch3. (b) Zhang, W.-H.; Chien, S. W.; Hor, T. S. A. Recent advances in metal catalysts with hybrid ligands. *Coord. Chem. Rev.* **2011**, *255*, 1991–2024.
- (15) Gogoll, A.; Örnebro, J.; Grennberg, H.; Bäckvall, J.-E. Mechanism of Apparent p-Allyl Rotation in (p-Allyl)-palladium Complexes with Bidentate Nitrogen Ligands. *J. Am. Chem. Soc.* **1994**, *116*, 3631–3632.
- (16) Basseti, M. Kinetic Evaluation of Ligand Hemilability in Transition Metal Complexes. *Eur. J. Inorg. Chem.* **2006**, 4473–4482.
- (17) (a) Ackermann, L. Carboxylate-Assisted Transition-Metal-Catalyzed C-H Bond Functionalizations: Mechanism and Scope. *Chem. Rev.* **2011**, *111*, 1315–1345. (b) Yang, Y.-F.; Hong, X.; Yu, J.-Q.; Houk, K. N. Experimental-Computational Synergy for Selective Pd(II)-Catalyzed C-H Activation of Aryl and Alkyl Groups. *Acc. Chem. Res.* **2017**, *50*, 2853–2860.
- (18) (a) Rousseaux, S.; Gorelsky, S. I.; Chung, B. K. W.; Fagnou, K. Investigation of the Mechanism of C(sp 3)-H Bond Cleavage in Pd(0)-Catalyzed Intramolecular Alkane Arylation Adjacent to Amides and Sulfonamides. *J. Am. Chem. Soc.* **2010**, *132*, 10692–10705 and references therein. (b) Zhang, B.-S.; Li, Y.; An, Y.; Zhang, Z.; Liu, C.; Wang, X.-G.; Liang, Y.-M. Carboxylate Ligand-Exchanged Amination/C(sp 3)-H Arylation Reaction via Pd/Norbornene Cooperative Catalysis. *ACS Catal.* **2018**, *8*, 11827–11833.
- (19) (a) Muzart, J. One-Pot Syntheses of α,β -Unsaturated Carbonyl Compounds through Palladium-Mediated Dehydrogenation of Ketones, Aldehydes, Esters, Lactones and Amides. *Eur. J. Org. Chem.* **2010**, 3779–3790. (b) Stahl, S. S. Palladium Oxidase Catalysis: Selective Oxidation of Organic Chemicals by Direct Dioxxygen-Coupled Turnover. *Angew. Chem., Int. Ed.* **2004**, *43*, 3400–3420.
- (20) (a) Gao, W.; He, Z.; Qian, Y.; Zhao, J.; Huang, Y. General palladium-catalyzed aerobic dehydrogenation to generate double bonds. *Chem. Sci.* **2012**, *3*, 883–886. (b) Zhang, J.; Jiang, Q.; Yang, D.; Zhao, X.; Dong, Y.; Liu, R. Reaction-activated palladium catalyst for dehydrogenation of substituted cyclohexanones to phenols and H $_2$ without oxidants and hydrogen acceptors. *Chem. Sci.* **2015**, *6*, 4674–4680.
- (21) Bergami, C.; Donzello, M. P.; Ercolani, C.; Monacelli, F.; Kadish, K. M.; Rizzoli, C. Tetra-2,3-pyrazinoporphyrazines with

Externally Appended Pyridine Rings. 3. A New Highly Electron-Deficient Octacationic Macrocyclic: Tetrakis-2,3-[5,6-di{2-(N-methyl)pyridiniumyl}pyrazino]porphyrazine, [(2-Me-py)₈TPyzPzH₂]⁸⁺. *Inorg. Chem.* **2005**, *44*, 9852–9861.